Supporting Information for

Controlled lanthanide-organic framework nanospheres as reversible and sensitive luminescent sensors approaching to practical applications

Yin-Ling Hou,[a,b] Hang Xu,[a] Rui-Rui Cheng,[a] and Bin Zhao*[,a]

[a] Department of Chemistry, Key Laboratory of Advanced Energy Material Chemistry, MOE, and Collaborative Innovation Center of Chemical Science and Engineering (Tianjin), Nankai University, Tianjin 300071, China.

[b] School of Chemistry and Materials Engineering, Kaili University, Kaili 556011 (China)

Corresponding Author

*E-mail： zhaobin@nankai.edu.cn.

Contents

1. Experimental Section

1.1 Materials and Physical Measurements

All chemicals were purchased commercially and used without further purification. Powder X-ray diffraction (PXRD) measurements were recorded on a D/Max-2500 X-ray diffractometer using Cu Kα radiation. The Fourier transform infrared (FT-IR) spectra were measured with a Bruker Tensor 27 spectrophotometer on KBr disks. The elemental analyses for C, H, and N were carried out by a Perkin-Elmer elemental analyzer. Thermogravimetric analyses were performed on a Netzsch TG 209 TG-DTA analyzer from room temperature to 800 ℃ under nitrogen atmosphere at heating rate of 10℃ min^{-1}. The emission spectra in the visible region were measured on a Cary Eclipse fluorescence spectrophotometer. The morphologies of the nano samples were observed by scanning electron microscopy (SEM, JEOL JSM7500F). High-resolution transmission electron microscopy (HRTEM) was obtained on a Tecnai G^2F20 system equipped.

1.2 Crystallographic Studies

Crystallographic data of **1** and **2** were collected on a SuperNova Single Crystal Diffractometer equipped with graphite-monochromatic MoKα radiation (λ = 0.71073 Å). The data integration and empirical absorption corrections were carried out by SAINT programs. All the structures were solved by direct methods and refined by full-matrix least-squares techniques based on F^2 using the SHELXS-97 and SHELXL-97 programs. [1] All the non-hydrogen atoms were refined with anisotropic parameters while H atoms were placed in calculated positions and refined using a riding model. The C2 and C3 atoms in compound **1** have been split into C2A, C2B and C3A, C3B, respectively, since they are disordered. ISOR instructions in SHELXL were imposed on C2A, C2B, C3A, C3B, C14, C20, C29, C34, N1, O20 and O21 atoms in compound **1**, and the DELU and SIMU instructions in SHELXL were imposed on N5 and C20 atoms get reasonable displacement parameters. The C1 atom in compound **2** have been split into C1A and C1B, and the DFIX instruction was used to fix the distance between C1A, N2 and C1B, N2. ISOR instructions in SHELXL were

imposed on O10, O19, O22 and C24 atoms in compound **2** to get reasonable displacement parameters. There are four large Q peaks around the Tb^{3+} ions (~1 Å) in compound **2**, which is from the series termination errors, and it also caused three B Alert-level. Crystallographic data for **1** and **2** were summarized in Table S1 (Supporting Information).

1.3 Synthesis

$\{[Eu_2(NO_3)_2(edc)(DMF)_4]\cdot 2DMF\}_n$ (1) and $\{[Tb_2(NO_3)_2(edc)(DMF)_4]\cdot DMF\cdot H_2O\}_n$ (2)

A mixture of 0.05 mmol H_4edc (0.0176 g), 0.1 mmol $Ln(NO_3)_3\cdot 6H_2O$ [Ln = Eu (0.0446 g), Tb (0.0453 g)], 3 mL EtOH, 1 mL DMF, and 0.5 mL H_2O was sealed in a glass vial (7 mL) and heated at 80 ℃ for 72 h under autogenous pressure. The vial was then cooled slowly down to room temperature at 1 ℃ h^{-1}. Needle crystals were obtained. The yield of **1** and **2** was 82% and 85% (based on $Ln(NO_3)_3\cdot 6H_2O$), respectively. Elemental analysis (%) for **1** ($C_{36}H_{52}N_8O_{22}Eu_2$), Calcd: C 35.41, H 4.18, N 8.94, Found: C 35.09, H 4.02, N 9.05; for **2** ($C_{33}H_{47}N_7O_{22}Tb_2$), Calcd: C 32.71, H 3.91, N 8.09, Found: C 32.96, H 4.12, N 7.83. IR (KBr, cm^{-1}): For **1**: 3422 (br), 1651 (s), 1588 (m), 1455 (w), 1386 (s), 1317 (w), 1266 (w), 1105 (w), 1070 (w), 1012 (w), 892 (w), 777 (m), 714 (w), 673 (w); For **2**: 3416 (br), 1657 (s), 1588 (m), 1456 (w), 1381 (s), 1317 (w), 1266 (w), 1110 (w), 1076 (w), 1007 (w), 898 (w), 782 (m), 714 (w), 678 (w).

Preparation of nanosphere 2 (NMOF-2)

The solid reactants in preparing **NMOF-2** are identical with that in the crystal **2**, and the differences are the concentration and the reaction time. Four different reactant concentrations (based on H_4edc at 10 mmol L^{-1}, 2 mmol L^{-1}, 1 mmol L^{-1} and 0.6 mmol L^{-1}) and four different reaction time (24 h, 48 h, 72h, and 6 d) were studied, and sixteen samples of **NMOF-2** were obtained. The reactants for different concentrations were sealed in a glass vial (7 mL) and heated at 80 ℃ under autogenous pressure for different time, and then the vial was taken out and cooled rapidly down to room temperature. A white suspension formed, which was rinsed

(centrifuged and dispersed in DMF) for several times before measurements. Here, the **NMOF-2** was obtained using solvothermal method without adding any seeds or surfactant, and the products were pure and easy to handle, which is the greatest advantage of this method. It should be noted that he surfactant-free solvothermal method for preparing NMOFs is rarely reported.[2]

2. Results and Discussin

2.1 Crystal Structures

Table S1. The crystal data of compounds **1** and **2**

Compound	**1** (Eu)	**2** (Tb)
Empirical formula	$C_{36}H_{52}N_8O_{22}Eu_2$	$C_{33}H_{47}N_7O_{22}Tb_2$
Formula weight	1252.78	1211.62
Temperature	122.5(8) K	122.20(10) K
Wavelength	0.71073 Å	0.71073 Å
Crystal system, space group	Triclinic, *P*-1	Triclinic, *P*-1
Unit cell dimensions	a = 13.2205(6) Å, α = 99.680(5)° b = 13.9973(8) Å, β = 91.009(4)° c = 14.9000(8) Å, γ = 117.103(5)°	a = 13.0090(10) Å, α = 99.513(4)° b = 13.7701(7) Å, β= 90.402(5)° c = 15.0439(7) Å, γ = 116.522(6)°
Volume	2405.5(2) Å^3	2368.1(2) Å^3
Z, Calculated density	2, 1.730 g cm^{-3}	2, 1.699 g cm^{-3}
Absorption coefficient	2.670 mm^{-1}	3.046 mm^{-1}
F(000)	1252.0	1200.0
Crystal size	0.22 × 0.19 × 0.18 mm	0.23 × 0.20 × 0.18 mm
2θ range for data collection	4.76 to 50.02°	4.72 to 50.02°
Limiting indices	-15 ≤ h ≤ 14, -16 ≤ k ≤ 16, -17 ≤ l ≤ 17	-15 ≤ h ≤ 15, -16 ≤ k ≤ 11, -17 ≤ l ≤ 17
Reflections collected / unique	14209 / 8406 [R(int) = 0.0268]	15291 / 8185 [R(int) = 0.0665]
Completeness to theta = 25.01	99.0%	97.9%
Data / restraints / parameters	8406 / 83 / 635	8185 / 374 / 606
Goodness-of-fit on F^2	1.070	1.045
Final R indices [I>2sigma(I)]	R_1[a] = 0.0377, wR_2[b] = 0.0780	R_1 = 0.0915, wR_2 = 0.2395
R indices (all data)	R_1 = 0.0477, wR_2 = 0.0842	R_1 = 0.1062, wR_2 = 0.2578

[a]$R_1 = \Sigma \parallel F_o| - |F_c \parallel / \Sigma|F_o|$ and [b]$wR_2 = \{\Sigma[w(F_o^2 - F_c^2)^2]/\Sigma[w(F_o^2)^2]\}^{1/2}$.

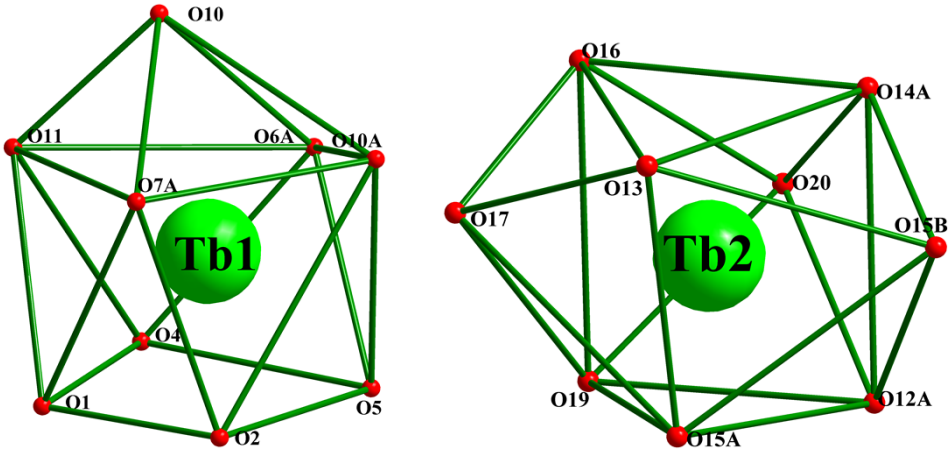

Fig. S1 The coordination geometries of Tb1 and Tb2 ions.

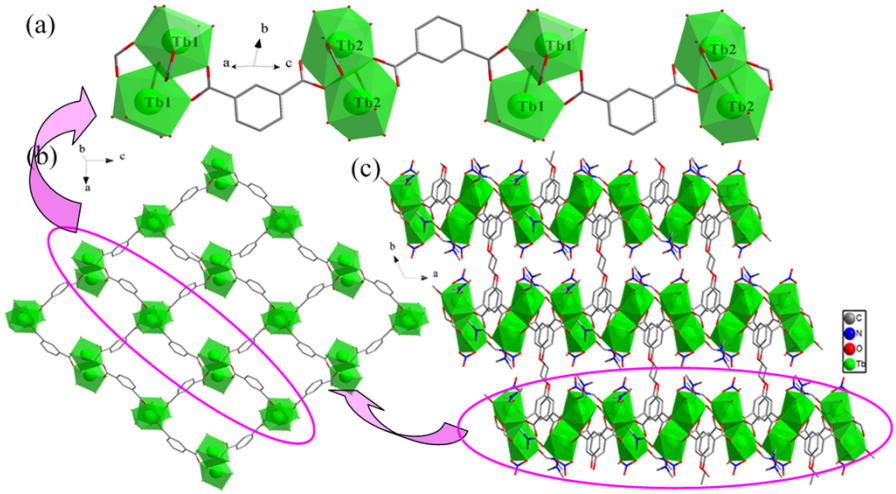

Fig. S2 The 1D chain (a), 2D layer (b), and 3D framework (c) of compound **2**.

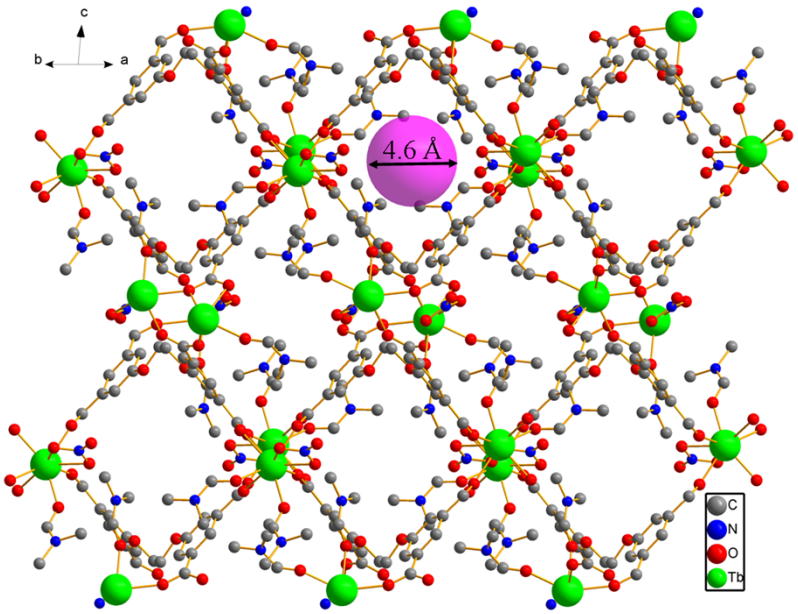

Fig. S3 The 3D framework structure of **2**, and the purple ball stands for the pore diameter in **2**.

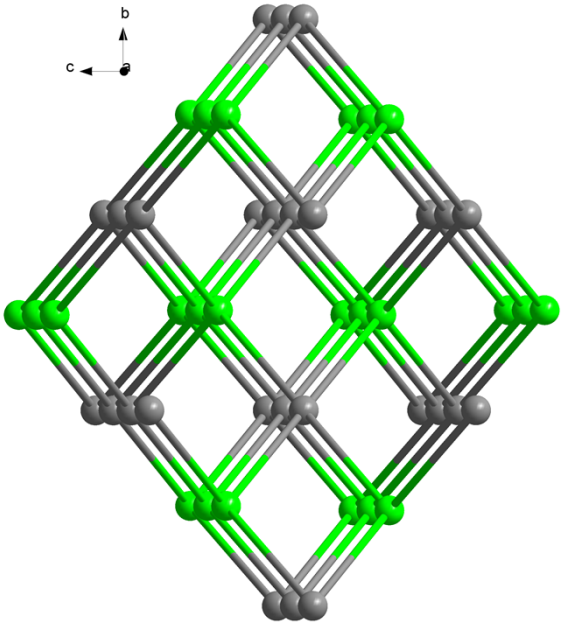

Fig. S4 The (4,4)-connected topological network of compound **2**, color codes: green, Tb^{3+}; gray, ligands.

2.2 The SEM of NMOF-2

The various sizes of **NMOF-2** were obtained by solvothermal reactions, and the nanocrystallines in Figs. S5-S8 are obtained by changing the reactant concentrations and reaction time. The **NMOF-2** in Figs. S5-S8 synthesized from concentration of H_4edc at 10, 2, 1 and 0.6 mmol L^{-1}, respectively. Under the concentration of H_4edc at 10 mmol L^{-1}, the sizes of the nanospheres have no marked difference in different reaction time, and the average diameter is about 1.1 μm, as shown in Fig. S5. The nanospheres of reaction time of 72 h are relatively uniform and pure, while the samples of reaction time of 24 h and 6 days have some unformed substances. We can conclude that under the concentration, 72 h is the optimized reaction time. However, under the reaction concentration of H_4edc at 2 mmol L^{-1}, the results are very good, and the sizes of the products with reaction time of 6 days are smaller, which is about 500 nm, while the other three samples have the similar size about 650 nm (Fig. S6). Under the concentration of H_4edc at 1 mmol L^{-1} and the reaction time of 24 h, the nanospheres are uniform with the average size of about 450 nm, as shown in Fig. S7. Continue to reduce the reaction concentration to 0.6 mmol L^{-1}, the smaller nanospheres were obtained with the average size of about 70 nm. Compared Figs. S5-

S8, we can safely conclude that the sizes of nanospheres significantly depend on the reaction concentration: lower concentration, smaller nanosphere.

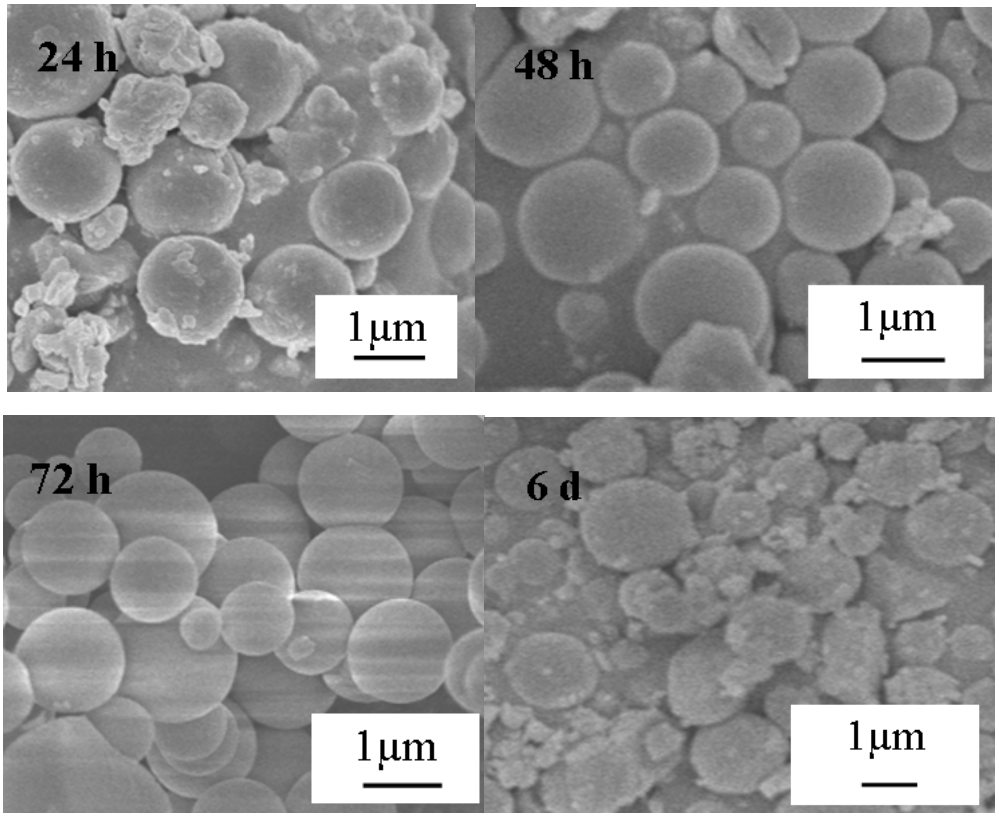

Fig. S5 SEM images of the **NMOF-2** synthesized under different reaction time and concentration of H_4edc at 10 mmol L^{-1}.

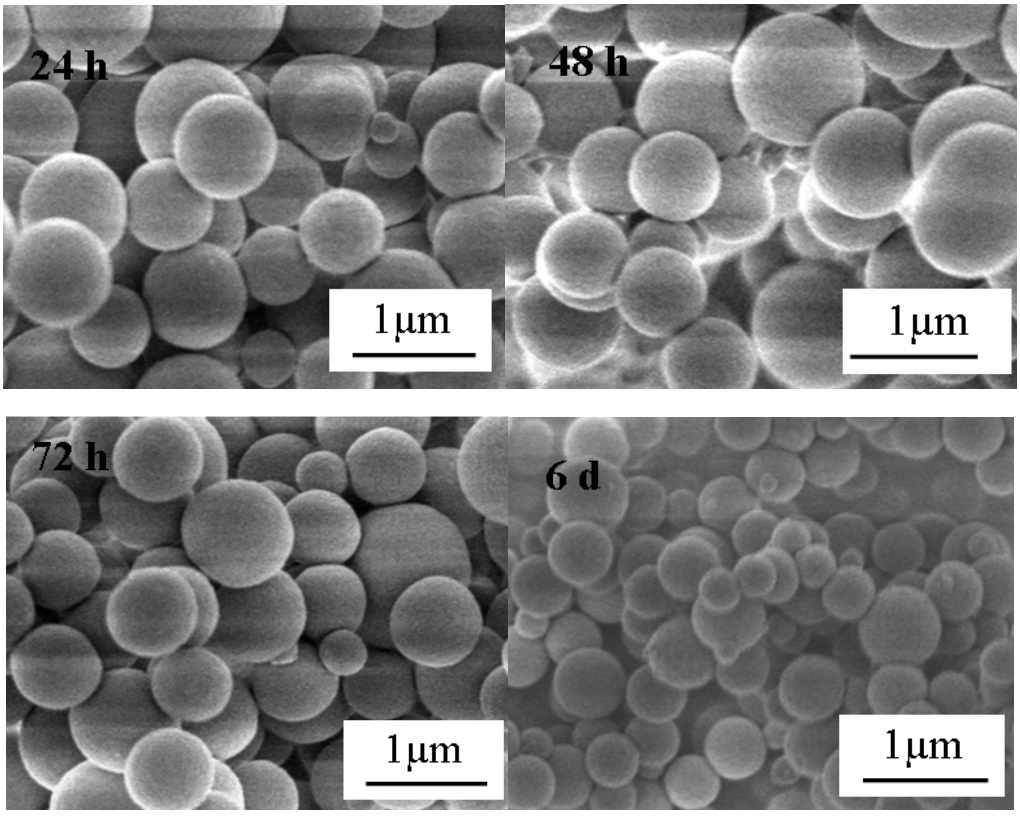

Fig. S6 SEM images of the **NMOF-2** synthesized under different reaction time and concentration of H_4edc at 2 mmol L^{-1}.

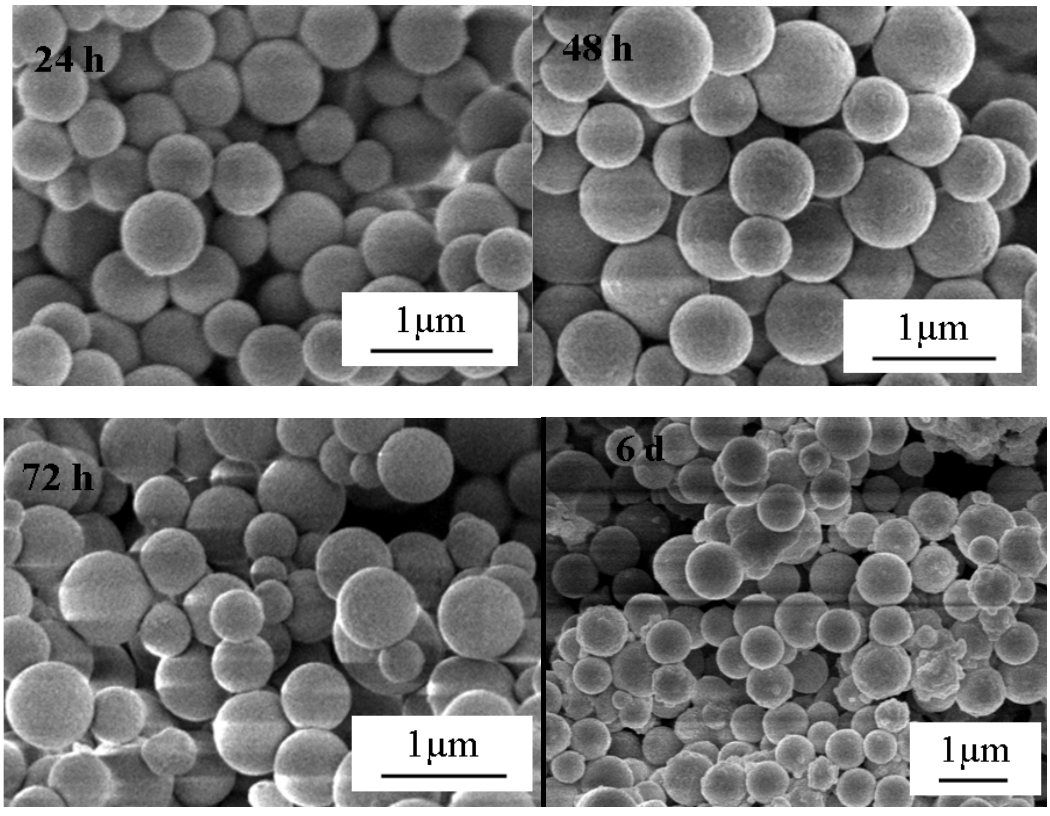

Fig. S7 SEM images of the **NMOF-2** synthesized under different reaction time and concentration of H_4edc at 1 mmol L^{-1}.

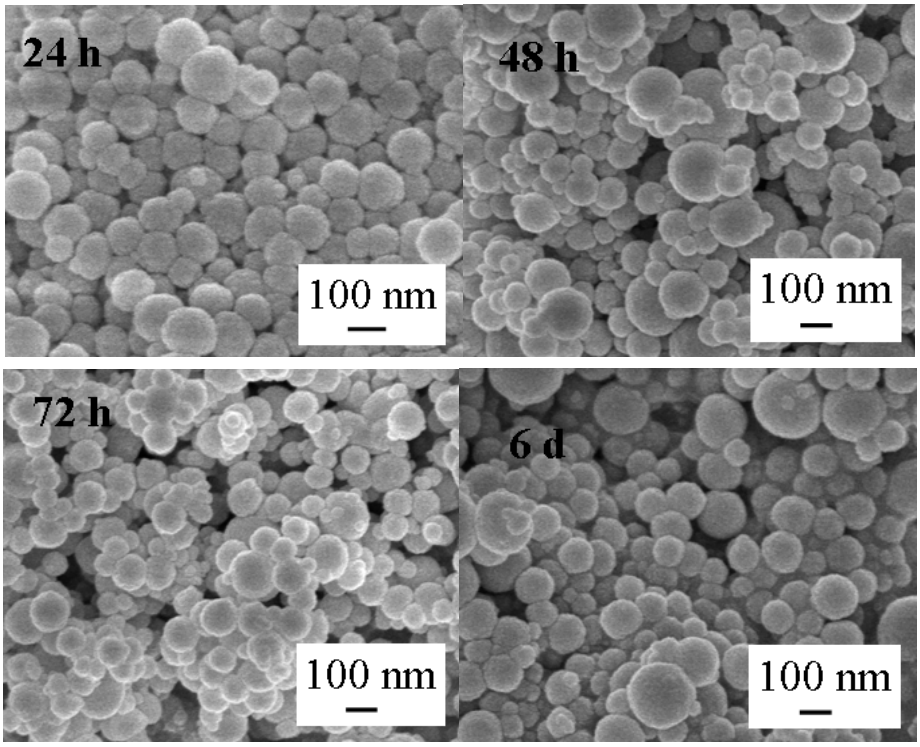

Fig. S8 SEM images of the **NMOF-2** synthesized under different reaction time and concentration of H_4edc at 0.6 mmol L^{-1}.

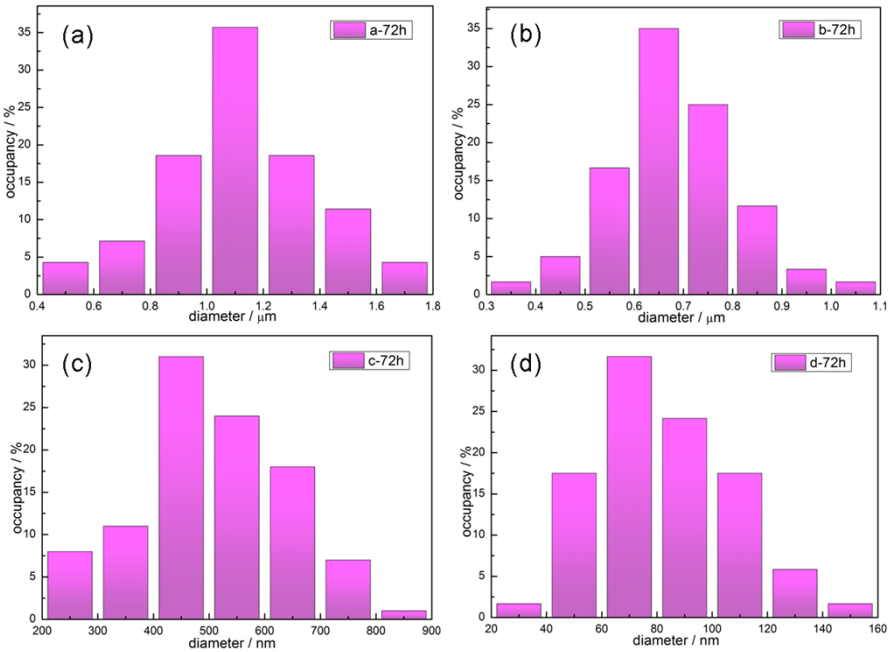

Fig. S9 Particle size distributions of **NMOf-2** formed in 72 h and the reaction concentration of 10 mmol L^{-1} (a), 2 mmol L^{-1} (b), 1 mmol L^{-1} (c), and 0.6 mmol L^{-1} (d), respectively.

2.3 IR, TG and PXRD Measurements

The IR spectra of the nanospheres obtained by the different reaction time were measured, as shown in Fig. S10, the peaks of the NMOFs overlapped the compounds **1** and **2**, suggesting the structures of NMOFs are the same with the compounds.

Further confirmation was carried out by the powder X-ray diffraction (PXRD), as shown in Fig. S11. The nano-powders obtained by reaction time of 24 h, 48 h, 72 h and 6d have the same structures with that of compound **2**, since the experimental PXRD patterns are well consistent with the simulated one obtained from the crystal data of **2**.

The purity of the compounds **1** and **2**, and the framework stability of the samples after immersed in different organic solvents were certified by the PXRD. As shown in Fig. S12, the experimental PXRD patterns of compounds **1** and **2** are agree with the corresponding simulated ones, indicating that the phase purity of the compounds is satisfactory.

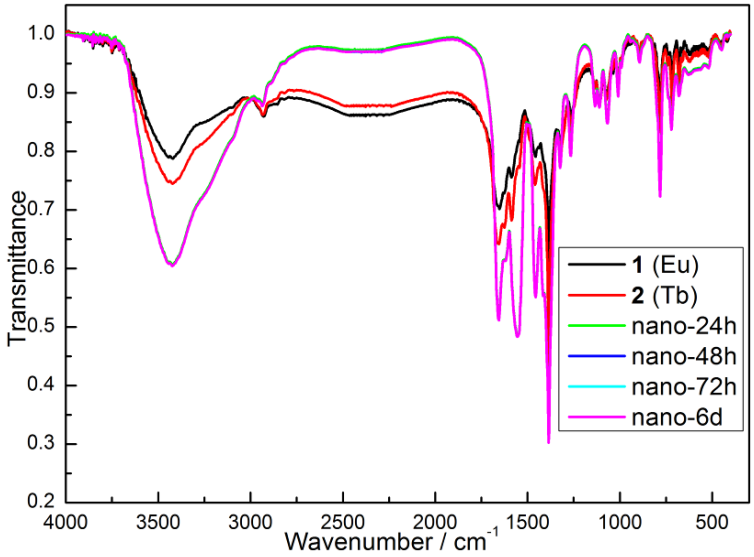

Fig. S10 The IR spectra of the compounds **1**, **2**, and the nanospheres obtained by different reaction time.

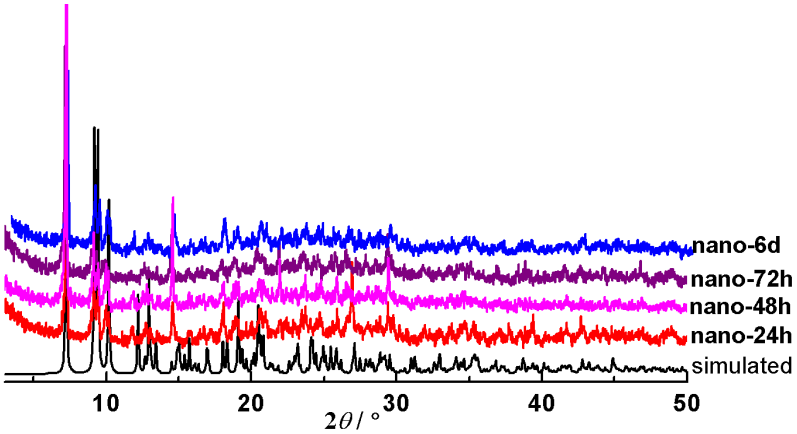

Fig. S11 The PXRD patterns of the **NMOF-2** under different reaction time and the simulated one obtained from the crystal data of **2**.

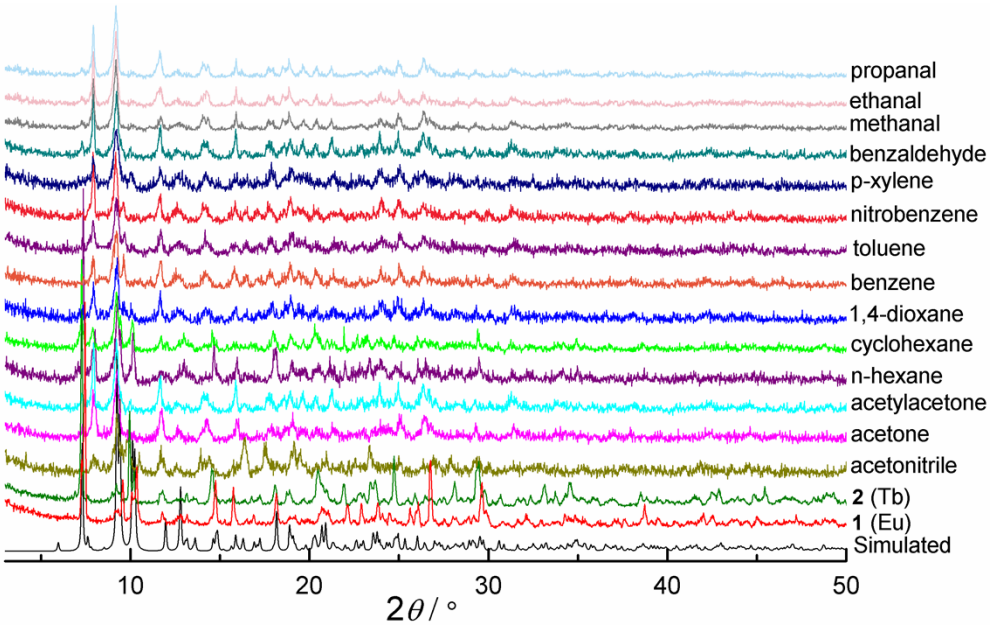

Fig. S12 The PXRD patterns of the simulated one from compound **2**, experiments of compounds **1** and **2**, and the compound **2** after immersed in different organic solvents for 24 h.

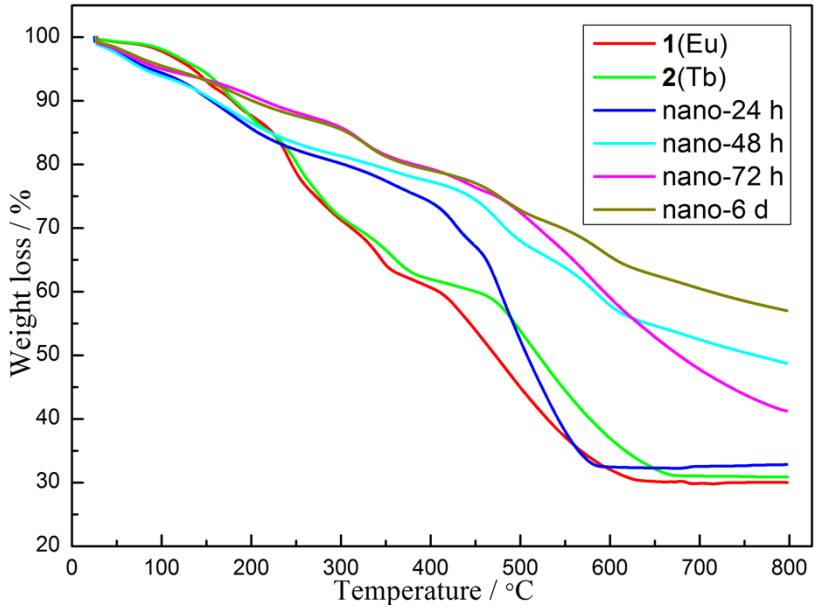

Fig. S13 The TGA curves of **2** (Tb) and the nanocrystallines obtained by different reaction time.

The thermal gravimetric analysis (TGA) of compounds **1** and **2**, and **NMOF-2** synthesized by different reaction time were conducted. As shown in Fig. S13, the TGA curves of compounds **1** and **2** are similar, since they are isostructural, so selecting compound **2** as the representation to describe the weight loss. Between room temperature and 170 ℃, the actual weight loss is about 8.37%, which closes to the theoretical value of 7.52%, corresponding to the loss of the guest molecules (one H_2O

and one DMF). Until to about 340 ℃, the experimental weight loss is about 32.28% (the calculated value is 31.65%), corresponding to the loss of the guest molecules and the four coordinated DMF molecules. And then the framework of **2** begins to collapse at about 400 ℃. For the **NMOF-2**, the more reaction time, the less weight loss. That maybe because as extending the reaction time, the nano-particles became more compact, and the guest molecules became less.

2.4 Luminescence Measurements

All of the luminescent emission spectra were measured on a Cary Eclipse fluorescence spectrophotometer. And assuring the measure conditions include the slit width of instrument, the position of the sample and the amount of the sample are uniform.

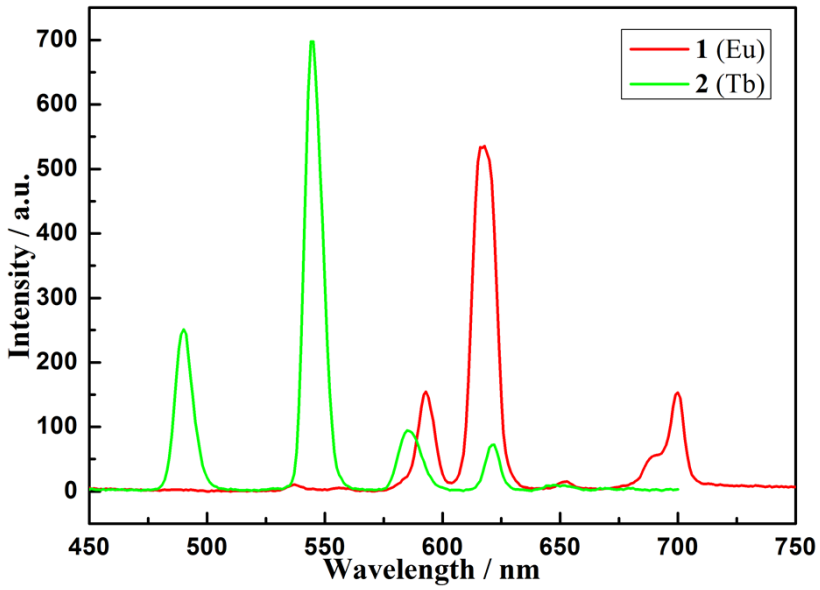

Fig. S14 The solid state luminescence of **1** and **2** at room temperature excited at 300 nm for **1** and 310 nm for **2**, respectively.

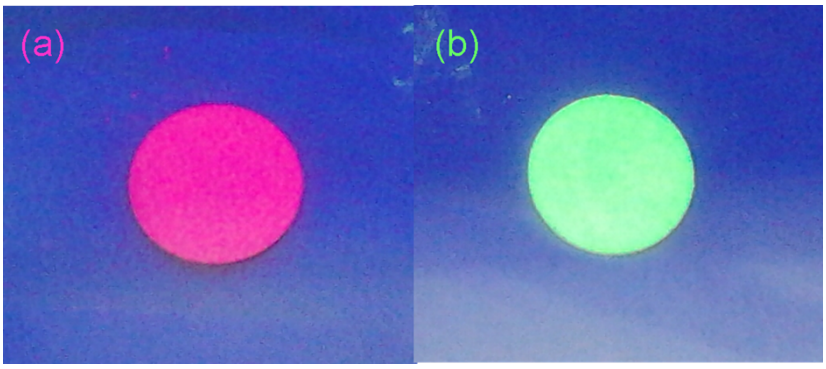

Fig. S15 The luminescence pictures of **1** (a) and **2** (b) under ultraviolet light, and the pictures are taken using a mobile phone.

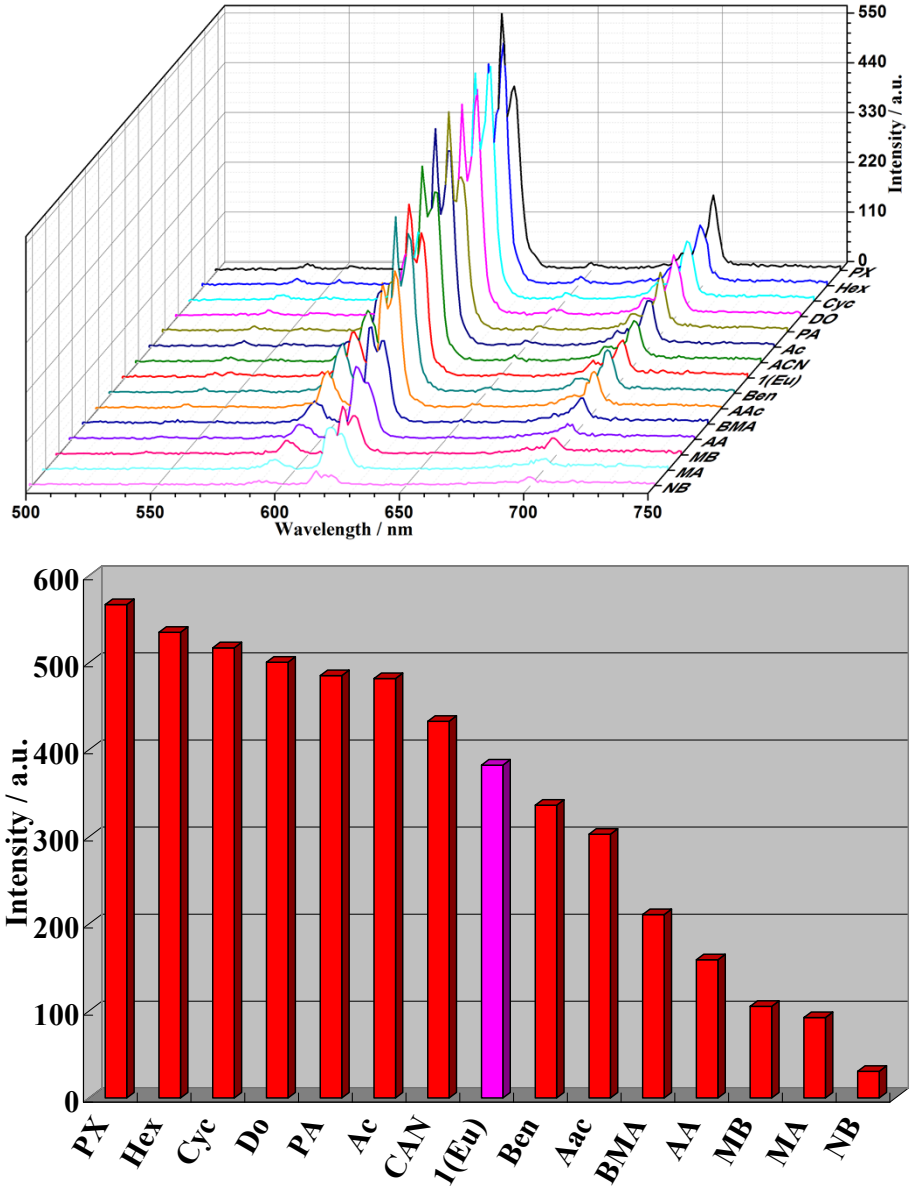

Fig. S16 (top) The luminescent intensities of **1** (Eu) after immersed in different organic solvents for 24 h; (bottom) The $^5D_0 \rightarrow {}^7F_2$ transition intensities of **1** (Eu) after immersed in different organic solvents for 24 h (excited at 300 nm).

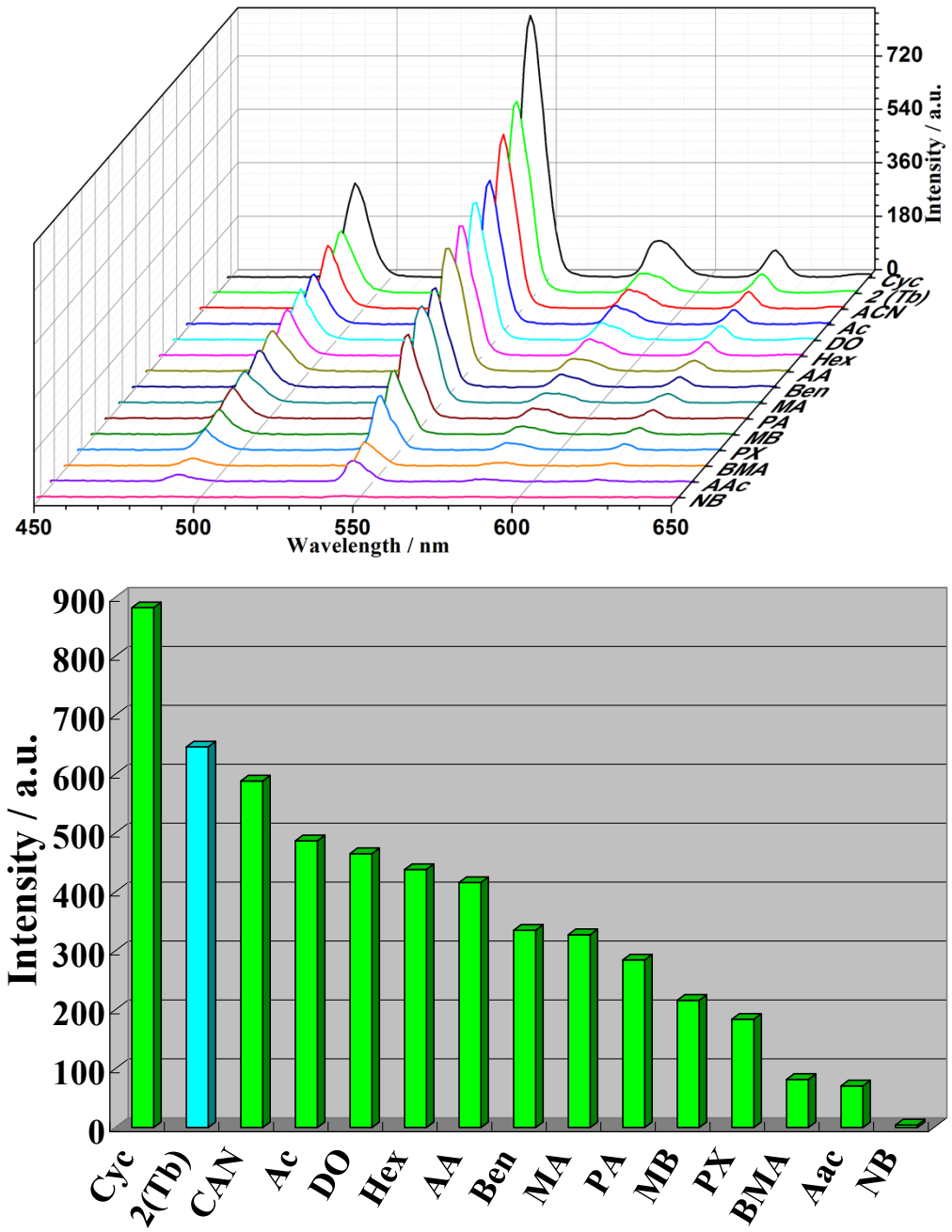

Fig. S17 The luminescent intensity of **2** (Tb) (top), and the $^5D_4 \rightarrow {}^7F_5$ transition intensity (bottom) after immersed in different organic solvents for 24 h (excited at 310 nm).

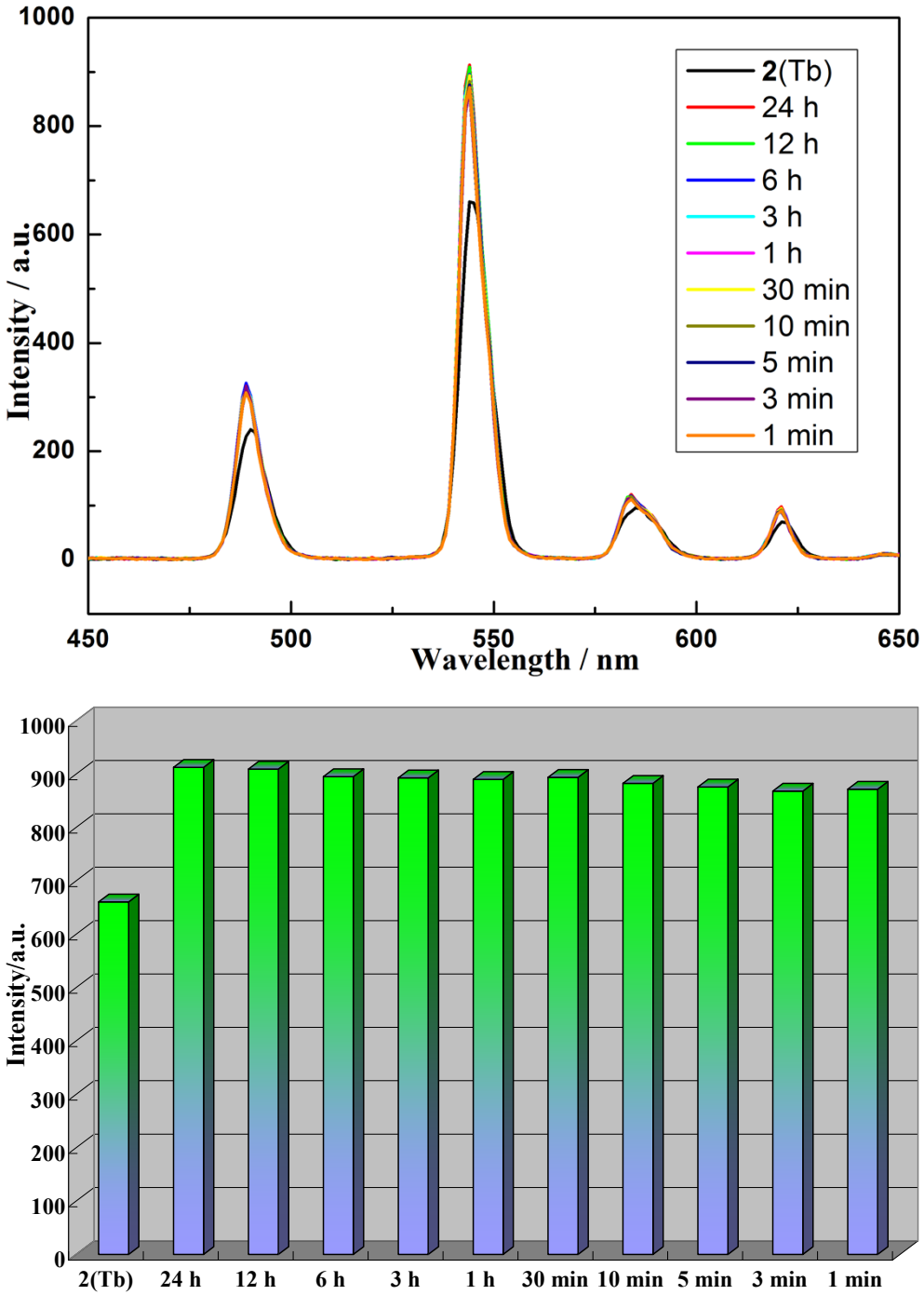

Fig. S18 (top) The luminescent intensities of **2** (Tb) after immersed in cyclohexane liquid for different time; (bottom) the $^5D_4 \rightarrow {}^7F_5$ transition intensities of **2** (Tb) after immersed in cyclohexane liquid for different time (excited at 310 nm).

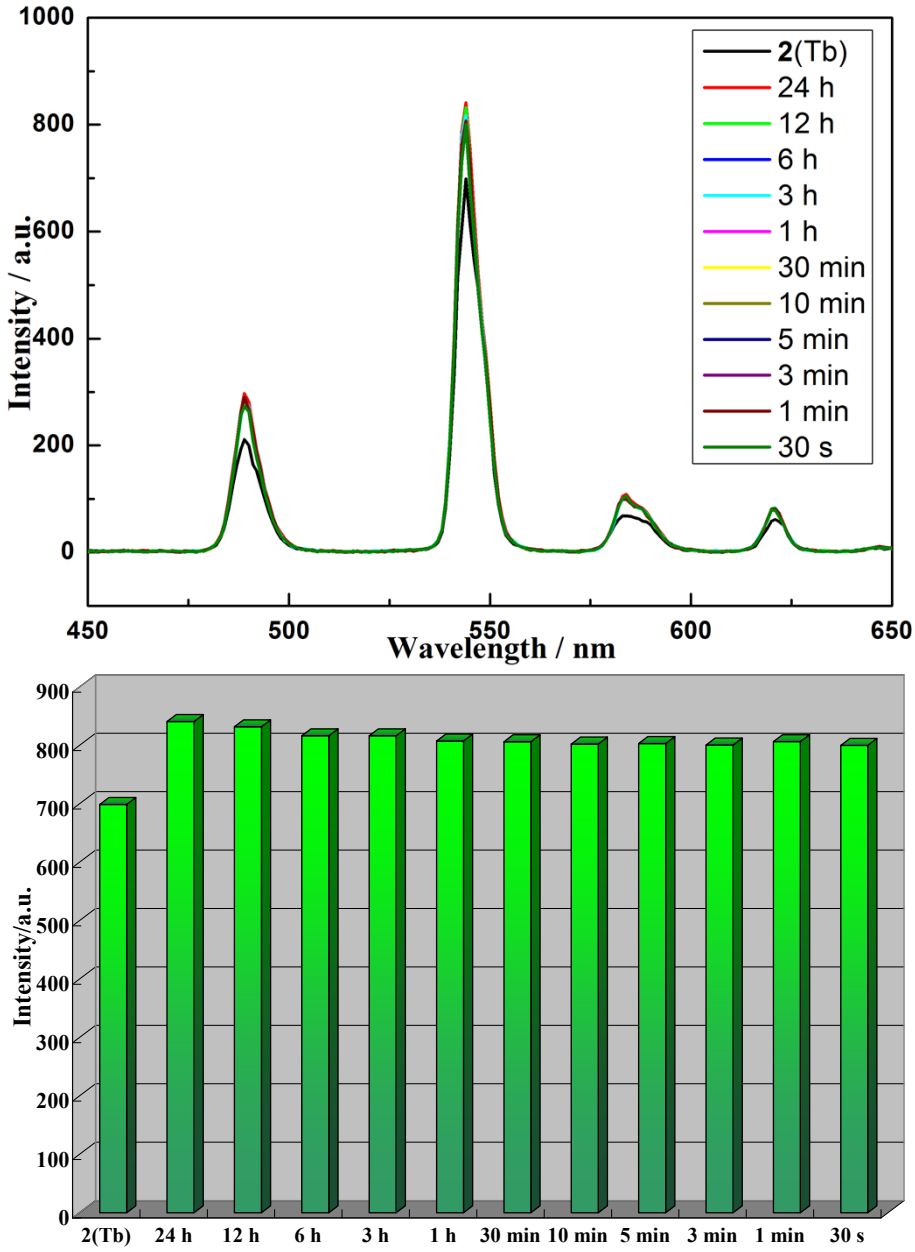

Fig. S19 (top) The luminescent intensities of **2** (Tb) after immersed in cyclohexane vapor for different time; (bottom) The $^5D_4 \rightarrow {}^7F_5$ transition intensities of **2** (Tb) after immersed in cyclohexane vapor for different time (excited at 310 nm).

In order to conveniently detect the influence of organic solvents on luminescent intensity, a self-made thin film device was constructed, as shown in Fig. S20. Glass sheets of dimension 1.35cm×2.5cm were first rinsed with distilled water and ethanol and then dried in air. A mixture of a certain proportion of the **NMOF-2** and N-methyl pyrrolidone (NMP) (100 mg: 1 mL) was thoroughly ground, and then adopting the dip-coating method to prepare the thin film. The thin film prepared by this method is dense and homogeneous.

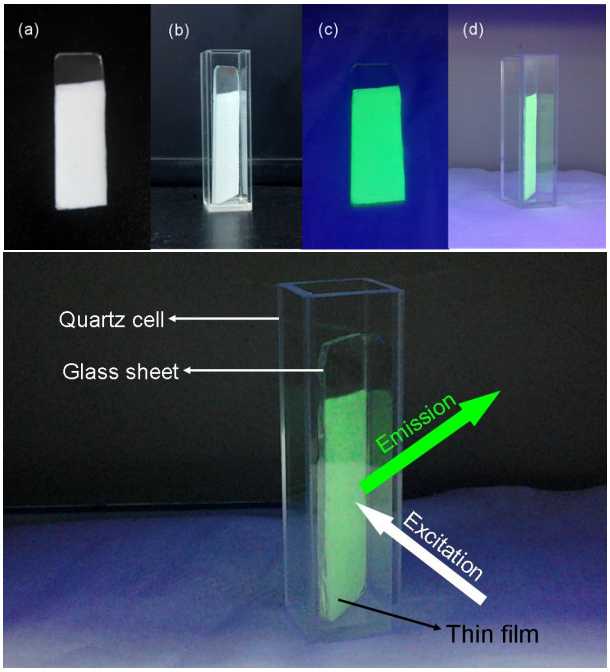

Fig. S20 The self-made thin film device for the detection of the changes of luminescent intensity caused by organic solvents.

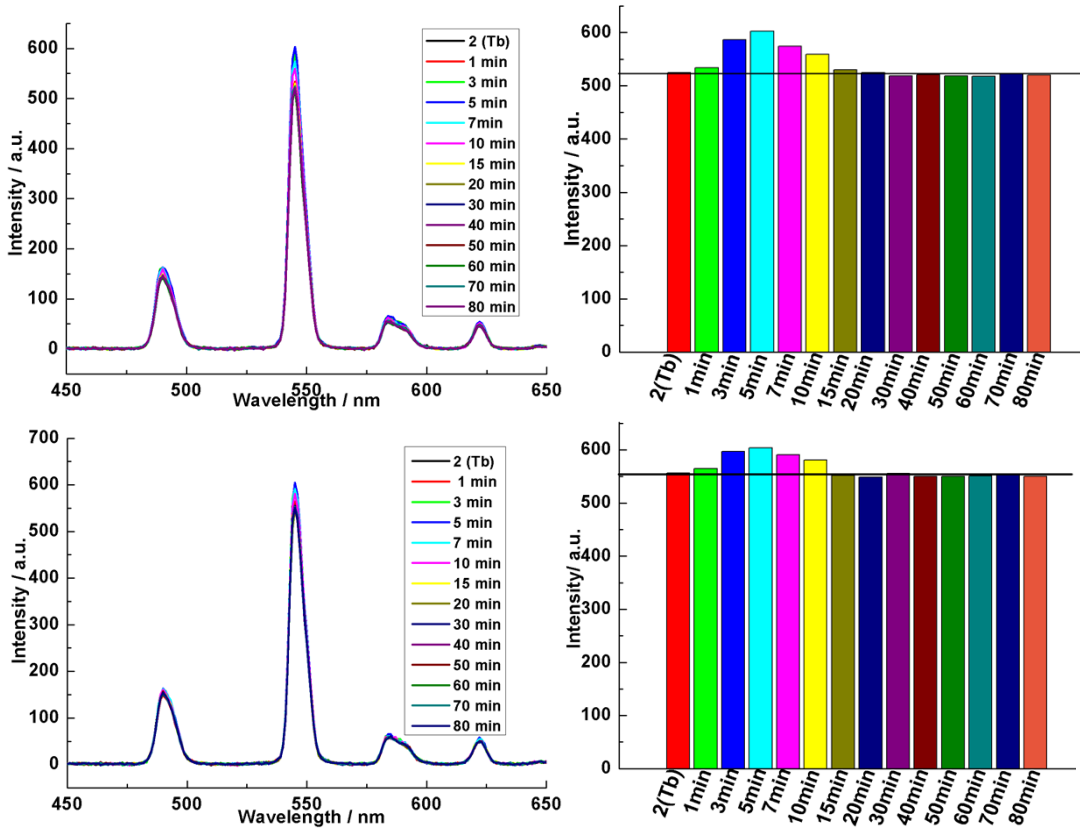

Fig. S21 The reversibility of the solid-state emission spectra of the thin film sample of **NMOF-2** in response to cyclohexane. The first cycle (top) and second cycle (bottom) for real-time monitoring upon adding one drop cyclohexane solvent.

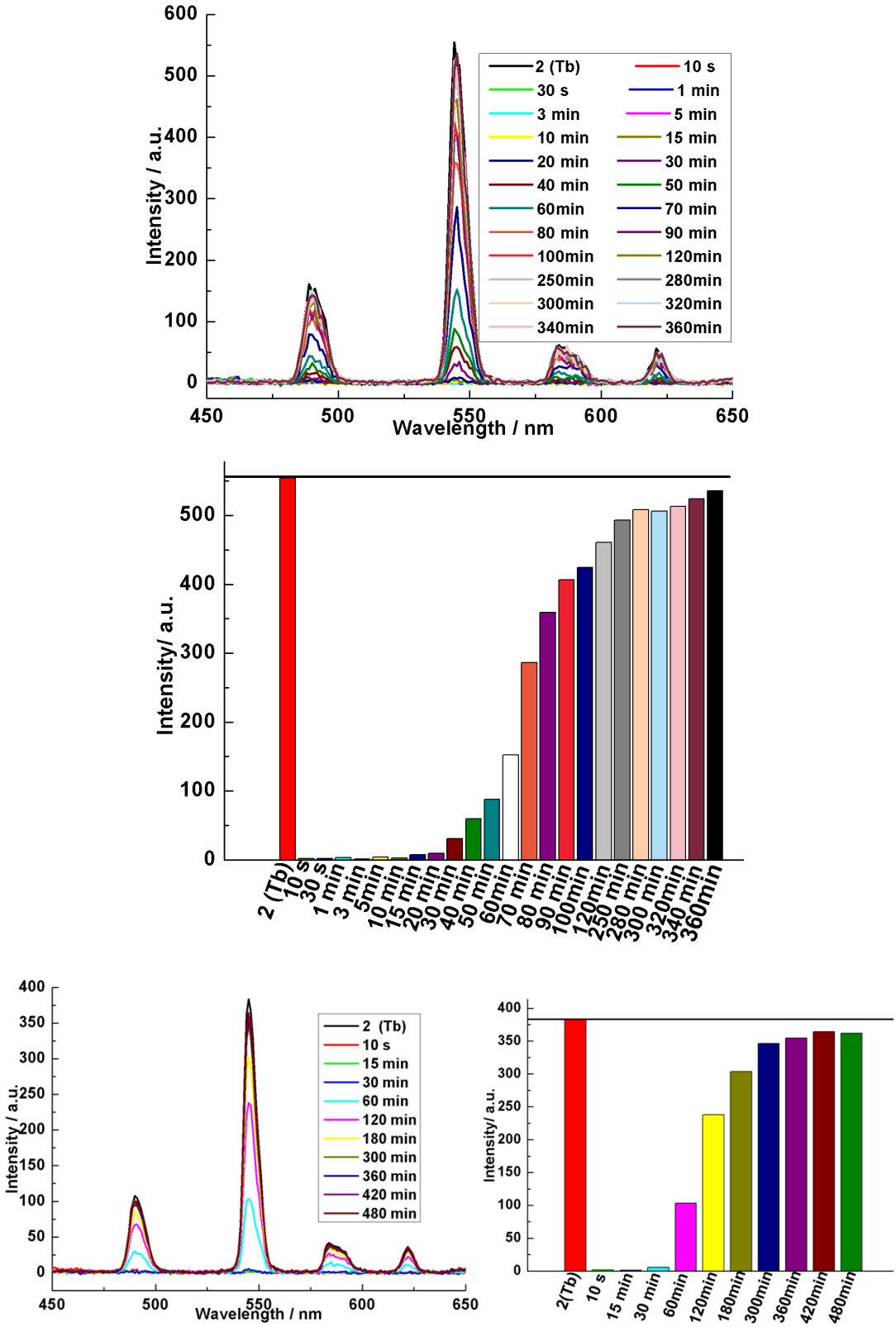

Fig. S22 The reversibility of the solid-state emission spectra of the thin film sample of **NMOF-2** in response to nitrobenzene. The first cycle (top and middle) and second cycle (bottom) for real-time monitoring upon adding 10 μL nitrobenzene solvent.

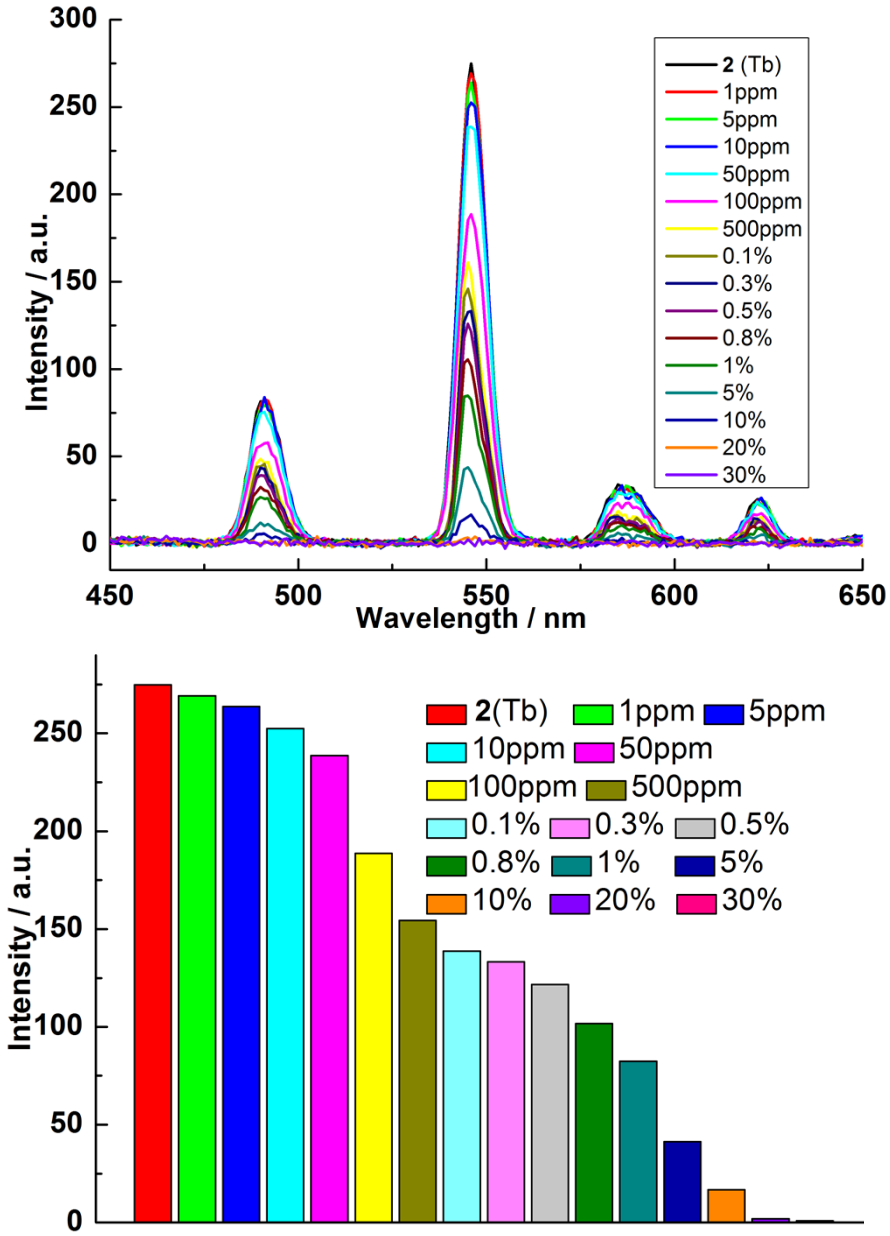

Fig. S23 (top) The quenching effect of different concentration of ethanol solutions of nitrobenzene; (bottom) The quenching of the $^5D_4 \rightarrow {}^7F_5$ transition intensity of the thin film samples of **NMOF-2** by different concentrations of nitrobenzene (excited at 310 nm).

The definition of quenching efficiency (QE) is: QE = $(I_0\text{-}I)/I_0 \times 100\%$,[3] where I_0 and I are luminescent intensity of the compound **2** before and after treated with nitrobenzene. And some quenching efficiency of different concentrations of nitrobenzene has been list in Table S2.

Table S2. The quenching efficiency of different concentrations of nitrobenzene

Concentration of nitrobenzene	10 ppm	50 ppm	100 ppm	500 ppm	0.1%	1%	10%
Quenching efficiency (%)	8.7	13.5	31.6	44.0	49.5	70.2	94.2

3. References

1 G. Sheldrick, *Acta Crystallogr., Sect. A*: Fundam. *Crystallogr*. 2008, **64**, 112.

2 (a) H. Xu, F. Liu, Y. J. Cui, B. L. Chen and G. D. Qian, *Chem. Commun*., 2011, **47**, 3153; (b) Y. P. Yuan, W. Wang, L. G. Qiu, F. M. Peng, X. Jiang, A. J. Xie, Y. H. Shen, X. Y. Tian and L. D. Zhang, *Mater. Chem. Phys*., 2011, **131**, 358; (c) S. B. Ding, W. Wang, L. G. Qiu, Y. P. Yuan, F. M. Peng, X. Jiang, A. J. Xie, Y. H. Shen and J. F. Zhu, *Mater. Lett*., 2011, **65**, 1385; (d) R. Li, Y. P. Yuan, L. G. Qiu, W. Zhang and J. F. Zhu, *Small*, 2012, **8**, 225; (e) Y. X. Xu, Y. Q. Wen, W. Zhu, Y. N. Wu, C. X. Lin and G. T. Li, *Mater. Lett*., 2012, **87**, 20; (f) B. V. Harbuzaru, A. Corma, F. Rey, P. Atienzar, J. L. Jordá, H. García, D. Ananias, L. D. Carlos and J. Rocha, *Angew. Chem. Int. Ed*., 2008, **47**, 1080; (g) A. Lan, K. Li, H. Wu, D. H. Olson, T. J. Emge, W. Ki, M. Hong and J. Li, *Angew. Chem. Int. Ed*., 2009, **121**, 2370; (h) C. Zhang, Y. Che, Z. Zhang, X. Yang and L. Zang, *Chem. Commun*., 2011, **47**, 2336; (i) Y. S. Xue, Y. B. He, L. Zhou, F. J. Chen, Y. Xu, H. B. Du, X. Z. You and B. L. Chen, *J. Mater. Chem. A*, 2013, **1**, 4525-4530.

3 (a) S. Pramanik, C. Zheng, X. Zhang, T. J. Emge and J. Li, *J. Am. Chem. Soc*., 2011, 133, 4153; (b) X. H. Zhou, H. H. Li, H. P. Xiao, L. Li, Q. Zhao, T. Yang, J. L. Zuo and W. Huang, *Dalton Trans.*, 2013, **42**, 5718.